

# Surface Modification of Low-Density Polyethylene Films by UV-Induced Graft Copolymerization and Its Relevance to Photolamination

Tie Wang, E. T. Kang,\* and K. G. Neoh

*Department of Chemical Engineering, National University of Singapore,  
Kent Ridge, Singapore 119260*

K. L. Tan

*Department of Physics, National University of Singapore, Kent Ridge, Singapore 119260*

D. J. Liaw

*Department of Chemical Engineering, National Taiwan University of Science and Technology,  
Taipei, Taiwan 106, Republic of China*

*Received September 8, 1997. In Final Form: November 24, 1997*

Surface modification of ozone-pretreated low-density polyethylene (LDPE) films were carried out via a novel technique of UV-induced graft copolymerization with acrylamide (AAM), Na salt of styrenesulfonic acid (NaSS), 3-dimethyl(methacryloyl)ethylammonium propanesulfonate (DMAPS), acrylic acid (AAc), *N,N*-dimethylacrylamide (DMAA), and 2-(dimethylamino)ethyl methacrylate (DMAEMA) under atmospheric conditions and in the complete absence of an added initiator or oxygen scavenger. Photografting with concurrent photolamination in assemblies containing a monomer solution sandwiched between two LDPE films was demonstrated. The chemical composition and microstructure of the graft copolymerized surfaces were studied by angle-resolved X-ray photoelectron spectroscopy. For LDPE films with high graft concentrations, such as those graft copolymerized with AAM, DMAA, and DMAEMA, surface chain rearrangement to form a stratified surface microstructure with a higher substrate to graft chain ratio at the outermost surface than in the subsurface layer was observed. The photolamination strengths depend on UV illumination time, monomer concentration, and the chemical nature of the monomer being graft copolymerized. Lap shear photolamination strength of about 90 N/cm<sup>2</sup> could be readily achieved in the LDPE/DMAPS(aq)/LDPE assembly after UV illumination. The failure mode of the photolaminated surfaces was either cohesive or adhesional in nature, depending on the type of monomer used in the photolamination assembly.

## Introduction

Surface modification of polymers via molecular design is one of the most versatile means of incorporating new functionalities into the existing polymers. These new functionalities have included improved surface hydrophilicity, hydrophobicity, biocompatibility, and adhesive properties,<sup>1–4</sup> just to name a few. Although a variety of physicochemical treatments have been applied to activate polymer surfaces, the surface grafting method has been regarded as an effective means for polymer surface functionalization during the past decade.<sup>5</sup> A fine approach to surface photografting of polymers was developed by Rånby et al.<sup>6,7</sup> In their process, the polymer substrates were irradiated by UV in a mixture of the monomer and photoinitiator.<sup>8–10</sup> During UV irradiation, the photoini-

tiators, such as benzophenone and its derivatives, are excited to a high-energy state which promotes abstraction of hydrogen from the polymer substrate. Thus, radicals are generated on the polymer surface for the subsequent initiation of graft copolymerization. Ikada et al.<sup>11–14</sup> on the other hand, have successfully incorporated a large number of functional groups onto polymer surfaces via graft copolymerization, usually in the absence of a photoinitiator. Prior to graft copolymerization, the polymer surfaces are pretreated with high-energy radiation, plasma, or ozone to introduce peroxides or hydroxyl peroxides, which are capable of initiating the subsequent graft copolymerization. The monomer solution must be purged with an inert gas or vigorously degassed to remove the dissolved oxygen. Alternatively, riboflavin and NaIO<sub>4</sub>

\* To whom correspondence should be addressed. Fax: (65) 779-1936. E-mail: cheket@nus.edu.sg.

(1) Brewis, D. M. *Surface and Pretreatment of Plastics and Metals*; Applied Science Publ.: London, 1982.

(2) Kinstle, J. F.; Watson, S. L., Jr. In *Polymer Alloys*; Klempner, D., Frisch, K. C., Eds.; Plenum Press: New York, 1977; p 461.

(3) Ikada, Y. *Biomaterials* **1994**, *15*, 725.

(4) Mittal, K. L., Ed. *Polymer surface Modification: Relevance to Adhesion*; VSP: Zeist, The Netherlands, 1995.

(5) Penn, L. S.; Wang, H. *Polym. Adv. Technol.* **1994**, *5*, 809.

(6) Rånby, B.; Gao, Z. M.; Hult, A.; Zhang, P. Y. *ACS Polym. Prepr.* **1986**, *27*, 38.

(7) Rånby, B. *J. Adhes. Sci. Technol.* **1995**, *9*, 599.

(8) Allmer, K.; Hult, A.; Rånby, B. *J. Polym. Sci., Part A: Polym. Chem.* **1988**, *26*, 2099.

(9) Zhang, P. Y.; Rånby, B. *J. Appl. Polym. Sci.* **1990**, *40*, 1647.

(10) Allmer, K.; Hult, A.; Rånby, B. *J. Polym. Sci., Part A: Polym. Chem.* **1988**, *27*, 1641.

(11) Uchida, E.; Uyama, Y.; Ikada, Y. *J. Polym. Sci., Part A: Polym. Chem.* **1989**, *27*, 527.

(12) Uchida, E.; Uyama, Y.; Ikada, Y. *J. Appl. Polym. Sci.* **1993**, *41*, 677.

(13) Mori, M.; Uyama, Y.; Ikada, Y. *J. Polym. Sci., Part A: Polym. Chem.* **1994**, *32*, 1683.

(14) Suzuki, M.; Kishida, A.; Iwata, H.; Ikada, Y. *Macromolecules* **1986**, *19*, 1804.

have been used in the monomer solution to consume the dissolved oxygen during exposure to UV light.<sup>11–15</sup>

More recently, an innovative bulk surface photografting process, in which a drop of solution containing the monomer and a photoinitiator was sandwiched between two thin films, has been reported.<sup>16–18</sup> Most importantly, photolamination occurred simultaneously during the photografting process, resulting in strong adhesion between the two films.<sup>19</sup> In a preliminary study carried out earlier, we demonstrated that simultaneous photografting and photolamination could be achieved in the complete absence of an added photoinitiator in the monomer when the polymer substrates were pretreated with ozone.<sup>20</sup> In addition, no system degassing or oxygen-removing agent, such as riboflavin or NaIO<sub>4</sub>, was required in this novel process, and surface graft copolymerization with concurrent photolamination proceeded readily under atmospheric conditions.

In the present study, detailed and systematic studies on the simultaneous surface photografting and photolamination are carried out with a variety of water-soluble monomers, such as acrylamide (AAM), acrylic acid (AAc), Na salt of styrenesulfonic acid (NaSS), 3-dimethyl(methacryloyl)ethylammonium propanesulfonate (DMAPS), *N,N*-dimethylacrylamide (DMAA), and 2-(dimethylamino)ethyl methacrylate (DMAEMA). Low-density polyethylene films are used as the substrate. The surface peroxides and hydroxyl peroxides species are generated from ozone pretreatment. The effects of UV-illumination time and monomer solution concentration used during photografting and photolamination on the lamination strengths are evaluated. The surfaces of the graft copolymerized films and the delaminated films after photolamination are characterized by angle-resolved X-ray photoelectron spectroscopy (XPS).

## Experimental Section

Commercial LDPE films of 0.125 mm in thickness were purchased from Goodfellow, Inc., of Cambridge, U.K. The surface of each film was cleaned by extractions with acetone and methanol before use. The AAc, AAM, NaSS, DMAA, and DMAEMA monomers were purchased from Aldrich Chemical Co. of Milwaukee, WI. The amphoteric DMAPS monomer was synthesized according to the method reported earlier.<sup>21</sup> All the monomers from the commercial source were used as received. The chemical structures and physical states at room temperature of the six monomers used in the present study are shown below:

acrylic acid (AAc):  $\text{CH}_2=\text{CHCOOH}$  (liquid)

acrylamide (AAM):  $\text{CH}_2=\text{CHCONH}_2$  (solid)

Na salt of styrenesulfonic acid (NaSS):

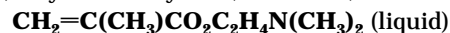


3-dimethyl(methacryloyl)ethylammonium propanesulfonate (DMAPS):



*N,N*-dimethylacrylamide (DMAA):  $\text{CH}_2=\text{CHCON}(\text{CH}_3)_2$  (liquid)

2-(dimethylamino)ethyl methacrylate (DMAEMA):



Ozone was generated in an ozone generator (Azcozon, Model RMU16-04EM) at an oxygen inlet flow rate of 60 L·h<sup>-1</sup> and an applied current of 0.4 A. The ozone production rate under these settings was about 2.5 g·h<sup>-1</sup>. The LDPE films were exposed to the oxygen–ozone gas mixture for 10 min in this study. This pretreatment time was chosen because ozone exposure time greater than 10 min could result in excessive oxidation of the LDPE surface. The latter phenomenon is apparent from the appearance of a significant amount of the C=O and COOH species in the XPS C 1s core-level spectra of LDPE surfaces with ozone treatment time greater than 10 min. A small quantity of the monomer solution of predetermined concentration was then introduced between the two ozone-pretreated LDPE films. The LDPE/monomer/LDPE assembly was sandwiched between two quartz plates by means of a mechanical clip before being illuminated by UV light. The UV source was provided by a Kratos LH 150w continuous xenon arc lamp. The light source has a calibrated intensity of about 10<sup>17</sup> photons/cm<sup>2</sup>·s in a 10 nm bandwidth in the spectral region of 290–400 nm. The lapped films were delaminated either by mechanical shearing or by soaking in hot water at 85 °C for 30 min. In the latter case, the self-delaminated films were subsequently washed with double-distilled water for an additional 24 h to remove the physically adsorbed homopolymer before being used for the investigation of surface graft copolymerization.

The LDPE films after graft copolymerization were characterized by angle-resolved XPS and water contact angle measurements. Water contact angles were measured at 25 °C and 50% relative humidity using a telescopic goniometer (Rame-Hart Model 100-00(230)). The telescope with a magnification power of 23× was equipped with a protractor of 1° graduation. The angles reported were reliable to ±3°.

XPS measurements were made on a VG ESCALAB MKII spectrometer with a Mg Kα X-ray source (1253.6 eV photons) at a constant retard ratio of 40. The polymer films were mounted on the standard sample studs by means of double-sided adhesive tape. The core-level signals were obtained at a number of photoelectron takeoff angles (α values measured with respect to sample surface), ranging from 20° to 75°. The X-ray source was run at a reduced power of 120 W (12 kV and 10 mA). The pressure in the analysis chamber was maintained at 7.5 × 10<sup>-9</sup> Torr or lower during each measurement. All binding energies (BEs) were referenced to the C 1s neutral carbon peak at 284.6 eV. In peak synthesis, the line width (full width at half-maximum or fwhm) for the Gaussian peaks was maintained constant for all components in a particular spectrum. Surface elemental stoichiometries were determined from peak-area ratios, after correcting with the experimentally determined sensitivity factors, and were reliable to ±5%. The elemental sensitivity factors were determined using stable binary compounds of well-established stoichiometries. The surface graft concentration of each polymer was expressed as the number of repeating units of the grafted chain per substrate carbon atom and was determined from the XPS-derived surface stoichiometries:

$$[\text{graft concentration}] = \frac{\text{number of repeating units of graft chain}}{\text{total number of substrate carbon}}$$

The lamination strengths were determined by measuring the lap shear adhesion strengths with a microprocessor-controlled miniature materials tester from the Rheometric Scientific, Inc., of U.K. The two lapped films were subjected to horizontal tensile stress at a crosshead speed of 0.1 cm/min. The tensile tests

(15) Zhang, J. F.; Kato, K.; Uyama, Y.; Ikada, Y. *J. Polym. Sci., Part A: Polym. Chem.* **1995**, *33*, 2629.

(16) Yang, W. T.; Rånby, B. *J. Appl. Polym. Sci.* **1996**, *62*, 533.

(17) Yang, W. T.; Rånby, B. *J. Appl. Polym. Sci.* **1996**, *62*, 545.

(18) Yang, W. T.; Rånby, B. *Macromolecules* **1996**, *29*, 3308.

(19) Yang, W. T. Lamination by Photografting. Ph.D. Thesis, Department of polymer Technology, Royal Institute of Technology, 10044 Stockholm, Sweden, 1996.

(20) Wang Tie; Lim, W. P.; Kang, E. T.; Neoh, K. G.; Fuh, J. Y. H.; Lu, L.; Nee, A. Y. C. *J. Adhes. Sci. Technol.* **1997**, *11*, 679.

(21) Liaw, D. J.; Lee, W. F. *J. Appl. Polym. Sci.* **1985**, *30*, 4697.

were carried out immediately after the photografting with concurrent lamination process. No attempts were made to remove the homopolymers coated on the outer surfaces of the lapped junction. For each lap shear strength reported, at least three sample measurements were averaged. The contact area of the films was kept at  $0.5\text{ cm} \times 0.1\text{ cm}$ , unless otherwise stated. The lapped area was kept small to prevent substrate yielding, especially in those cases in which high adhesion strengths were achieved.

## Results and Discussion

**1. Surface Graft Copolymerization.** The surface graft copolymerized films used for surface characterization were obtained from various self-delaminated LDPE/monomer/LDPE assemblies in water after the UV-induced graft copolymerization with concurrent photolamination under atmospheric conditions. The fact that the photolaminated films are susceptible to self-delamination in water would suggest that the two LDPE films were not directly connected by the graft chains to a significant extent.

Parts a and d of Figure 1 show the respective C 1s core-level and wide scan spectra, obtained at  $\alpha$  values of  $75^\circ$  and  $20^\circ$ , for an ozone pretreated LDPE film after having been subjected to UV-induced simultaneous graft copolymerization and photolamination in the presence of a small quantity of 10 wt % AAm monomer solution for 30 min. The presence of surface-grafted Aam polymer can be deduced from the presence of the C 1s core-level component at the binding energy (BE) of 287.7 eV, attributable to the  $\text{CONH}_2$  species.<sup>22</sup> A lower graft yield (lower  $\text{CONH}_2$  component intensity) is obtained for the back substrate, as a result of the attenuated UV light intensity reaching this substrate (see also below). The C 1s component at the BE of 285.8 eV, on the other hand, is probably associated with the surface-oxidized carbon species, such as the C–O species, arising from the UV-induced graft copolymerization. An earlier study<sup>20</sup> has shown that the 10 min of ozone pretreatment alone under similar conditions gives rise to a much less intense C–O component signal in the LDPE film. Comparison of the  $\text{CONH}_2$  components intensities in the C 1s core-level spectra and the N 1s/C 1s peak intensity ratios in the wide scan spectra at the two  $\alpha$  values readily reveals the presence of a higher substrate to graft chain ratio at the more surface glancing angle of  $20^\circ$  for this heavily grafted surface. The angular-dependent XPS results thus suggest that the hydrophilic AAm polymer graft chains must have become submerged beneath a thin surface layer, which is richer in the substrate chains than the subsurface layer, to form a stratified surface microstructure. In addition, the top surface of the graft-modified LDPE substrate suffers a greater extent of surface oxidation, as suggested by the presence of a higher intensity of the C–O component at 285.8 eV for the spectrum obtained at  $\alpha = 20^\circ$ .

Figure 2 shows the respective C 1s core-level and wide scan spectra, obtained at  $\alpha$  values of  $75^\circ$  and  $20^\circ$ , for a 10 min ozone pretreated LDPE film after having been subjected to UV-induced graft copolymerization and photolamination in 10 wt % NaSS monomer solution for 30 min. The C 1s component at the BE of 284.6 eV is associated with the carbon atoms of the surface-grafted styrenesulfonic acid polymer (as no Na 1s signal is detected) and that of the LDPE substrate chain. The C–O component is again associated with the surface oxidation process, similar to that observed in the Aam graft copolymerized LDPE film. However, the stratified surface

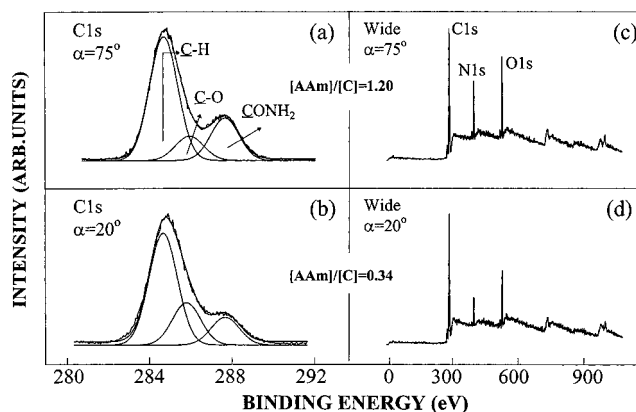


**Figure 1.** Angular-dependent (a) and (b) C 1s core-level and (c) and (d) wide scan spectra, for the 10-min ozone-pretreated LDPE film after graft copolymerization in 10 wt % Aam monomer solution.

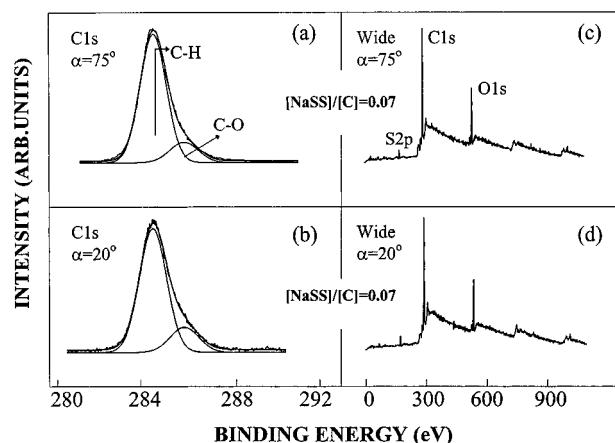


**Figure 2.** Angular-dependent (a) and (b) C 1s core-level, and (c) and (d) wide scan spectra, for the 10-min ozone-pretreated LDPE film after graft copolymerization in 10 wt % NaSS monomer solution.

microstructure is not observed in this case due to the low graft yield of the NaSS polymer, as indicated by the wide scan spectra.

Similar surface microstructures are observed for LDPE films at both high and low extents of surface graft copolymerization with DMAA, DMAEMA, and DMAPS. The respective angle-resolved C 1s core-level spectra for the front and backside LDPE films after graft copolymerization in 10 wt % DMAA solution are shown in Figure 3. The corresponding spectra obtained from graft copolymerization in 10 wt % DMAEMA solution are shown in Figure 4. The C 1s core-level spectra of the DMAA graft copolymerized LDPE surfaces are curve-fitted with three peak components with BEs at 284.6 eV for the C–H species, 285.8 eV for the N–CH<sub>3</sub> and C–O species, and 287.5 eV for the  $\text{CON}(\text{CH}_3)_2$  species.<sup>23,24</sup> Similarly, the C 1s core-level spectra of DMAEMA graft copolymerized LDPE in Figure 4 are also curve-fitted with three peak components with BE's at 284.6 eV for the C–H species, 286.0 eV for the N–CH<sub>3</sub> and C–O species, and 288.4 eV for the COO species.<sup>25</sup> The stratified surface microstructure is not observed in this case, as a result of lower graft

(22) Kang, E. T.; Neoh, K. G.; Tan, K. L.; Uyama, Y.; Morikawa, N.; Ikada, Y. *Macromolecules* **1992**, *25*, 1959.

(23) Kang, E. T.; Neoh, K. G.; Chen, W.; Tan, K. L.; Huang, C. C.; Liaw, D. J. *J. Adhes. Sci. Technol.* **1996**, *10*, 725.

(24) Kang, E. T.; Tan, K. L.; Kato, K.; Uyama, Y.; Ikada, Y. *Macromolecules* **1996**, *29*, 6872.

(25) Kang, E. T.; Neoh, K. G.; Tan, K. L.; Loh, F. C.; Liaw, D. J. *Polym. Adv. Technol.* **1993**, *5*, 837.

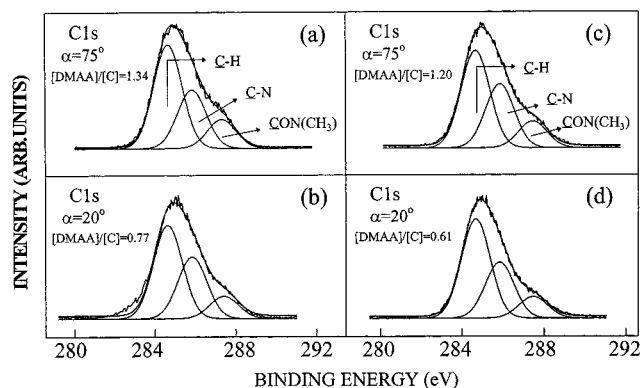


**Figure 3.** Angular-dependent C 1s core-level spectra of (a) and (b) the front and (c) and (d) the back LDPE films of the LDPE/DMAA/LDPE assembly after delamination by soaking in hot water ( $O_3$  pretreatment time = 10 min, UV illumination time = 10 min).

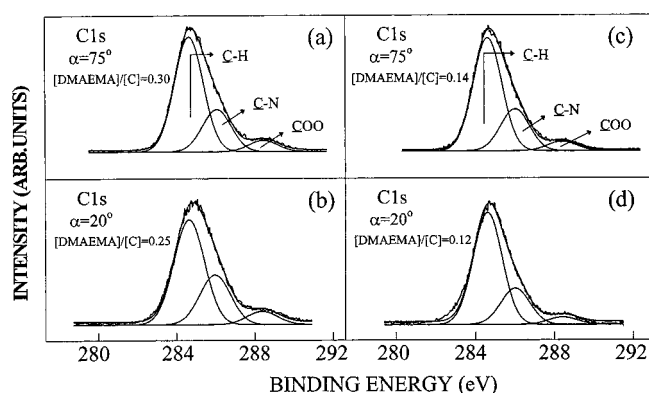


**Figure 4.** Angular-dependent C 1s core-level spectra of (a) and (b) the front and (c) and (d) the back LDPE films of the LDPE/DMAEMA/LDPE assembly after delamination by soaking in hot water ( $O_3$  pretreatment time = 10 min, UV illumination time = 10 min).

yield for the DMAEMA polymer. In either Figure 3 or Figure 4, it is also observed that the graft yield in the front film is higher than that in the back. The asymmetry in surface concentrations of the grafted DMAA and DMAEMA chains on the two self-delaminated surfaces must have resulted from the attenuated UV light intensity reaching the back substrate.<sup>20</sup>

Parts a–d of Figure 5 show the angular-dependent C 1s core-level and wide scan spectra of an LDPE film after graft copolymerization in 10 wt % DMAPS solution under the same conditions as those of the previous cases. The corresponding N 1s and S 2p core-level spectra, obtained at  $\alpha = 75^\circ$ , for the film are shown in parts e and f of Figure 5, respectively. As shown in parts a and b of Figure 5, the C 1s core-level spectra can be curve-fitted with three peak components with BEs at 284.6 eV for the C–H species, 286.2 eV for the combination of C–O and C–N species, and 288.5 eV for the COO species. Nitrogen was not discernible in the wide scan spectra due to its low concentration and sensitivity factor. The N 1s and S 2p core-level spectra consist of a single peak component with BEs at 402.3 eV for the  $N^+$  species and 168.1 eV for the  $SO_3^-$  species, respectively.<sup>26</sup> Similar to the results obtained in Figure 2, the stratified surface microstructure is not observed in the present case. The relatively low graft yield in the two cases probably arises from steric hindrance due to the existence of bulky substituent in

**Table 1.** Water Contact Angles of LDPE Film after Surface Graft Copolymerization with AAc, AAm, NaSS, DMAPS, DMAA, and DMAEMA<sup>a</sup>

	monomer concn (%)	contact angle (deg)
AAc	5	52
	10	40
AAm	5	47
	10	22
NaSS	5	53
	10	42
DMAPS	5	57
	10	53
DMAA	5	37
	10	35
DMAEMA	5	41
	10	35

<sup>a</sup> The water contact angle for pristine LDPE is  $99^\circ$ .

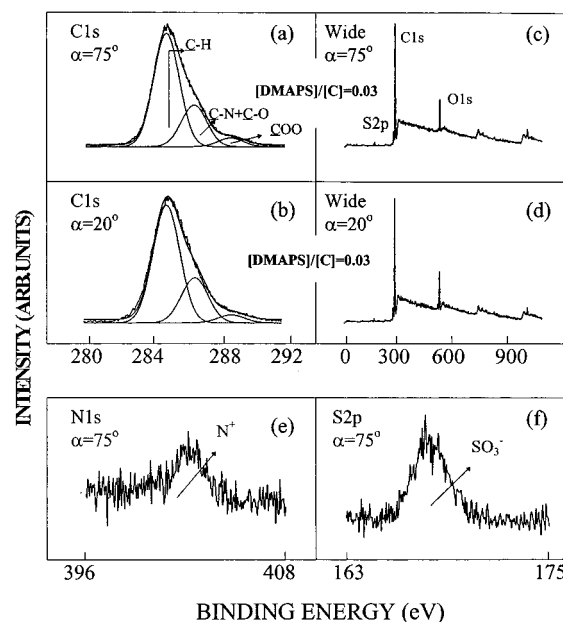


**Figure 5.** Angular-dependent (a) and (b) C 1s core-level, and (c) and (d) wide scan spectra, and (e) N 1s and (f) S 2p spectra, obtained at  $\alpha = 75^\circ$ , for the 10-min ozone-pretreated LDPE film after graft copolymerization in 10 wt % DMAPS monomer solution.

each monomer. Finally, the surface concentration of grafted AAc polymer from the simultaneous photografting and lamination in the LDPE/10 wt % AAc/LDPE assembly was in the order of 0.22, when measured at  $\alpha = 75^\circ$ , for the front film.

Graft copolymerization with the various water-soluble monomers also gives rise to hydrophilic LDPE surfaces, as indicated by the significant decrease in water contact angles for all the graft-modified films in Table 1. In general, an increase in monomer concentration readily gives rise to a higher graft concentration and results in a more hydrophilic LDPE surface.

**2. Photolamination.** The effects of monomer concentrations on the photolamination strengths between two ozone-pretreated LDPE films are shown in Figure 6 and Figure 7, respectively, for the liquid and solid monomers. The insert in Figure 6 shows schematically the entanglement of the photografted chains at the lapped junction which contributes to the observed lamination phenomenon. In the cases of liquid monomers (AAc, DMAA, and DMAEMA), the lap shear adhesion strengths increase with the liquid monomer concentrations, as shown in Figure 6. In each case, the highest photolamination strength is obtained when pure monomer is used. On the

(26) Chastain, J., Ed. *Handbook of X-ray Photoelectron Spectroscopy*; Perkin-Elmer: Eden Prairie, MN, 1992.

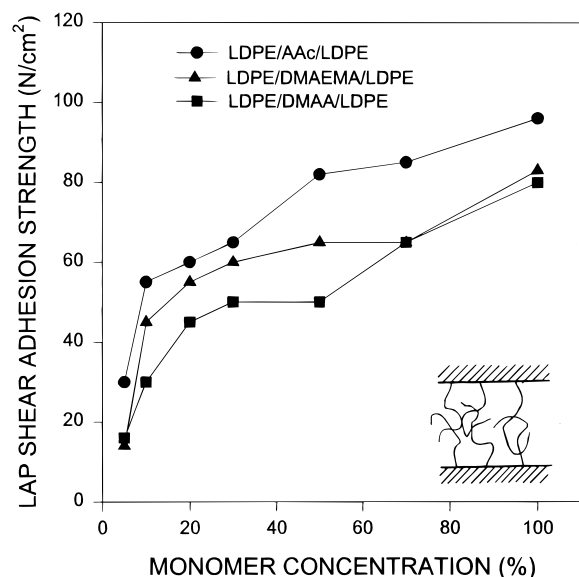


**Figure 6.** Effect of monomer concentration on the development of photolamination strength of the LDPE/AAc/LDPE, LDPE/DMAA/LDPE, and LDPE/DMAEMA/LDPE assemblies ( $O_3$  pretreatment time = 10 min, UV illumination time = 30 min). The contribution of the photografted chains to the observed lamination phenomenon is illustrated schematically in the insert.

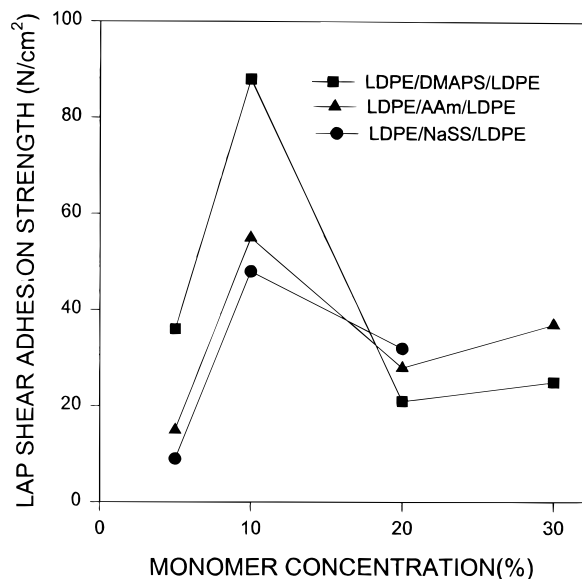


**Figure 7.** Effect of monomer concentration on the development of photolamination strength of the LDPE/AAm/LDPE, LDPE/NaSS/LDPE, and LDPE/DMAPS/LDPE assemblies ( $O_3$  pretreatment time = 10 min, UV illumination time = 30 min).

other hand, maximum lap shear strengths are obtained at about 10 wt % aqueous monomer concentration for all three solid monomers (NaSS, DMAPS, and AAm) studied, as shown in Figure 7. The latter phenomenon is not well understood but may have been associated with the presence of unreacted solid monomers at high monomer concentrations. The evaporation of the solvent (water) and the accompanied precipitation or phase separation of the unreacted monomer at the interface when high monomer concentrations are used may have caused a substantial reduction in the lamination strength. In the cases of the liquid monomers, the excess or unreacted monomer either can evaporate simultaneously with the solvent or can participate in the subsequent bulk polym-

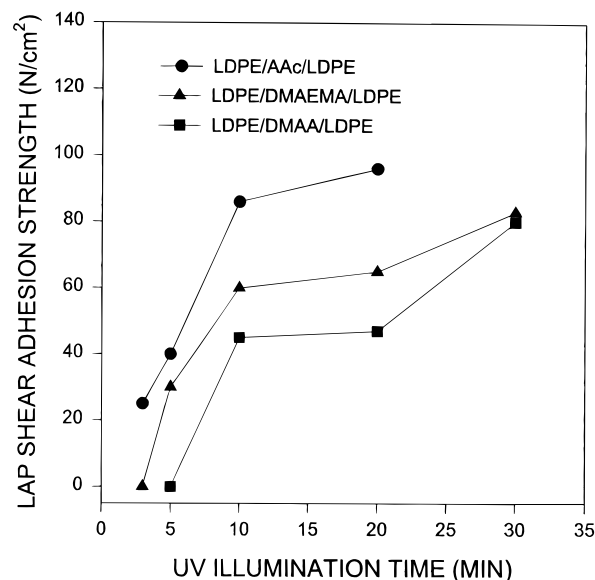


**Figure 8.** Effect of UV illumination time on the development of photolamination strength of the LDPE/AAc/LDPE, LDPE/DMAA/LDPE, and LDPE/DMAEMA/LDPE assemblies ( $O_3$  pretreatment time = 10 min, monomer concentration = 100%).

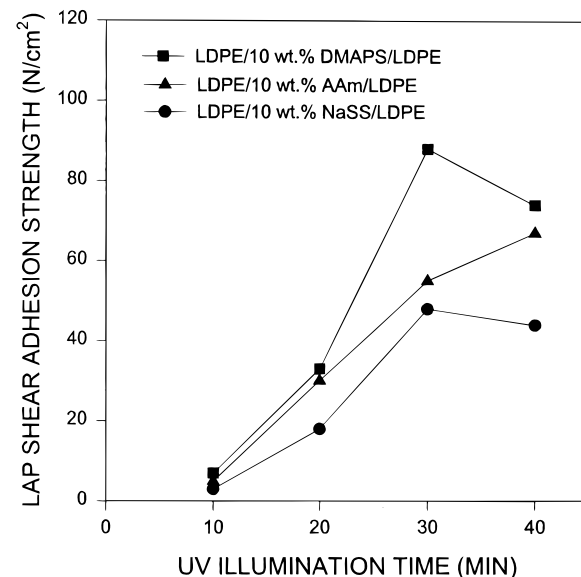


**Figure 9.** Effect of UV illumination time on the development of photolamination strength of the LDPE/10 wt % AAm/LDPE, LDPE/10 wt % NaSS/LDPE, and LDPE/10 wt % DMAPS/LDPE assemblies ( $O_3$  pretreatment time = 10 min).

erization, resulting in the gradual and continuous increase in lamination strength.

On the basis of the above observations, assemblies fabricated with pure liquid monomers and with 10 wt % solutions of the solid monomers were used to determine the effects of UV illumination time on the photolamination strengths. Figure 8 and Figure 9 summarize the effects of UV illumination time on the photolamination strength of the liquid and the solid monomer systems, respectively. As shown in Figure 8, both the rate and adhesion strength of photolamination for the LDPE/AAc/LDPE assembly are significantly higher than those of the LDPE/DMAA/LDPE and LDPE/DMAEMA/LDPE assemblies. The ultimate lamination strength of the LDPE/AAc/LDPE assembly approaches 100 N/cm<sup>2</sup> when pure AAc monomer is used. These results probably arise from the high polymerization rate of the AAc monomer and the high bulk strength of

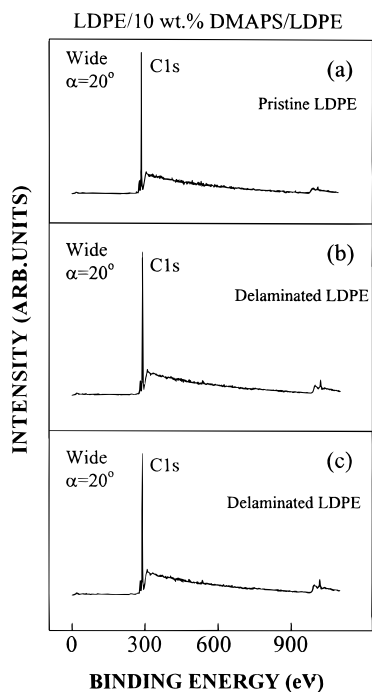


**Figure 10.** Wide scan spectra, obtained at  $\alpha = 20^\circ$ , for (a) a pristine LDPE film and (b) and (c) the delaminated surfaces of the LDPE films from the LDPE/DMAPS/LDPE assembly.

the Aac polymer. The relatively low adhesion strengths observed for the LDPE/DMAA/LDPE assemblies, despite of the high graft yield of DMAA polymer, would suggest the presence of relatively short graft chains and/or the presence of steric hindrance among the DMAA polymer chains at the interface. In the cases of the solid monomers in Figure 9, the adhesion strengths increase rapidly with UV-illumination time up to about 30 min, after which the adhesion strengths either increase at a much slower rate (the LDPE/10 wt % AAm/LDPE assembly) or decrease slightly (the LDPE/10 wt % DMAPS/LDPE and the LDPE/10 wt % NaSS/LDPE assemblies). Relatively poor lamination behavior is observed for the LDPE/10 wt % NaSS/LDPE assembly, as suggested by the relatively low lap shear adhesion strengths obtainable. The poor lamination strengths observed can be attributed to the relatively poor grafting efficiency of the NaSS polymer on LDPE, as shown in Figure 2. On the other hand, a strong lamination strength is observed for the LDPE/10 wt % DMAPS/LDPE assembly, as suggested by the achieved lap shear adhesion strength of about 90 N/cm<sup>2</sup> after 30 min of UV illumination. The low graft yield of the DMAPS polymer on LDPE does not seem to provide a strong support for the strong lamination strength observed. This discrepancy can probably be accounted for by the unique chemical properties of the DMAPS polymer (Figure 9). As DMAPS is an amphoteric monomer, i.e., containing both the cation ( $-N^+$ ) and anion ( $-SO_3^-$ ) groups in its chemical structure, strong interchain and intrachain charge-transfer interactions between the cation  $N^+$  and anion  $SO_3^-$  species can occur when entanglement of the grafted DMAPS polymer chains on the two LDPE film surfaces takes place during the simultaneous grafting and lamination process. Despite the higher graft yield, the LDPE/10 wt % AAm/LDPE assembly exhibits an adhesion strength significantly below that of the LDPE/10 wt % DMAPS/LDPE assembly. Therefore, the photolamination strengths are not governed just by the graft concentration but also by the nature of the interactions among the graft chains.

The failure modes of the above six photolaminated

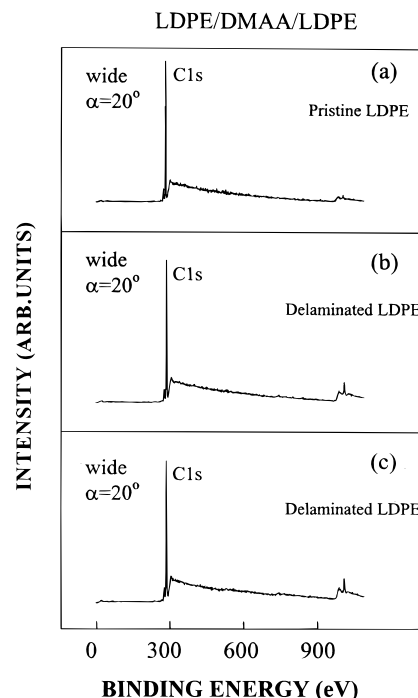


**Figure 11.** Wide scan spectra, obtained at  $\alpha = 20^\circ$  for (a) a pristine LDPE film and (b) and (c) the delaminated surfaces of the LDPE films from the LDPE/DMAA/LDPE assembly.

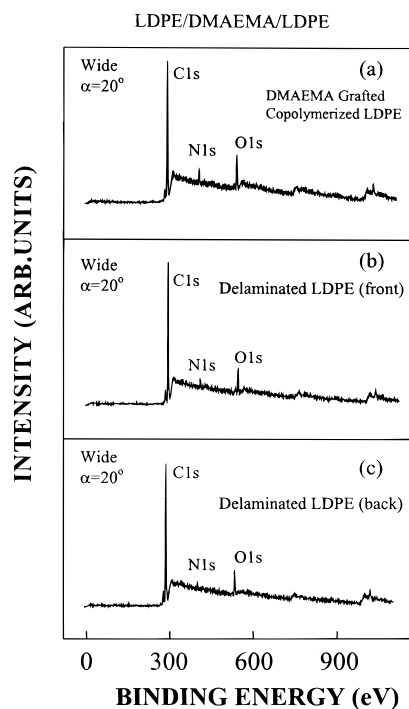


**Figure 12.** Wide scan spectra, obtained at  $\alpha = 20^\circ$ , for (a) a DMAEMA graft copolymerized LDPE film surface and (b) the front and (c) the back LDPE films delaminated from the LDPE/DMAEMA/LDPE assembly.

assemblies (with 30 min of UV illumination time) after mechanical shearing were also investigated. The wide scan spectra, obtained at  $\alpha = 20^\circ$ , for the two delaminated LDPE films from the LDPE/10 wt % DMAPS/LDPE assembly are shown in parts b and c of Figure 10. The features of both spectra are similar to those of the pristine LDPE film shown in Figure 10a. Thus, the XPS results suggest that the two delaminated surfaces are essentially similar to that of the pristine LDPE film. This result

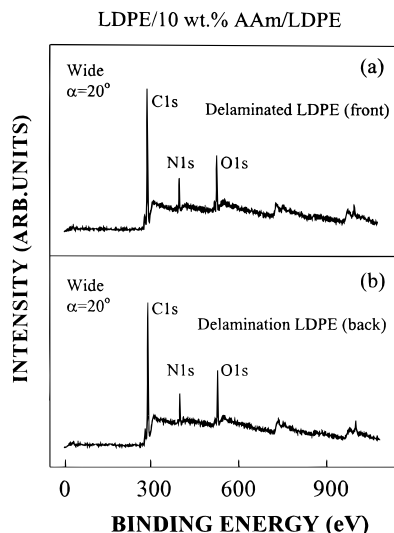


**Figure 13.** Wide scan spectra, obtained at  $\alpha = 20^\circ$ , for (a) the front and (b) the back LDPE films delaminated from the LDPE/AAm/LDPE assembly.

clearly indicates that the failure mode of the photolaminated LDPE films in the presence of 10 wt % DMAPS solution is cohesive in nature and takes place in the bulk or below the graft–substrate interface of either film. Similar results are also observed in Figure 11 for the delaminated LDPE/DMAA/LDPE assembly. Cohesive failure has also been observed for the LDPE/AAC/LDPE assembly.<sup>20</sup> In all these cases, the graft chains have been completely removed from the LDPE surfaces during the mechanical shearing process.

Figures 12–14 show the respective wide scan spectra, obtained at  $\alpha = 20^\circ$ , for the two delaminated film surfaces from the remaining three assemblies. As shown in parts b and c of Figure 12, the wide scan spectra for the delaminated surfaces of the LDPE/DMAEMA/LDPE assembly remain similar to that of the DMAEMA graft copolymerized LDPE film shown in Figure 12a, except for the fact that the nitrogen signal for the backside film is somewhat reduced. This result suggests that the lamination failure of the LDPE/DMAEMA/LDPE assembly must have involved the fracture of the DMAEMA chains in the interface between the two laminated LDPE films. Figure 13 shows the XPS wide scan spectra, obtained at  $\alpha = 20^\circ$ , for the delaminated films from the LDPE/10 wt % AAm/LDPE assembly after mechanical shearing. The wide scan spectra and the amounts of nitrogen are similar to that of the AAm graft copolymerized LDPE films (Figure 1d). This result again suggests that the failure mode of the two photolaminated LDPE films from graft copolymerization with AAm must have also involved the fracture of the grafted AAm polymer chains on each surface, rather than below it. (Initially, the graft chains from both surfaces entangled in the interfacial region to provide for

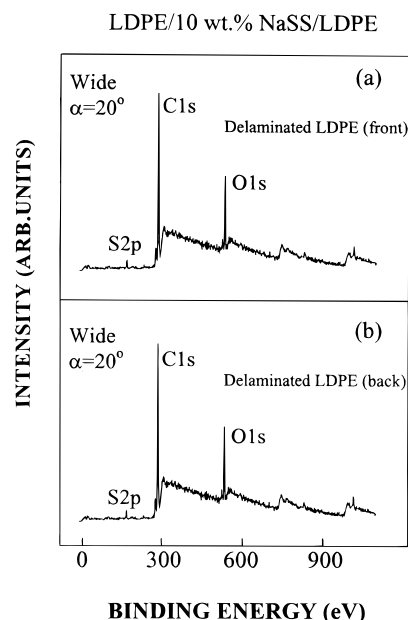


**Figure 14.** Wide scan spectra, obtained at  $\alpha = 20^\circ$ , for (a) the front and (b) the back LDPE films delaminated from the LDPE/NaSS/LDPE assembly.

the observed adhesion strength.) Similar XPS results are also observed for the delaminated LDPE/10 wt % NaSS/LDPE assembly, as shown in Figure 14. Thus, the failure mode of the last three assemblies can be regarded as “adhesional failure”. By taking into account of the ultimate photolamination strengths of the various assemblies, it appears that cohesive failure is associated with high lamination strengths, while adhesional failure arises from weaker junctions.

### Conclusion

Surface photografting induced laminations between two LDPE films with a variety of monomers were investigated. The graft copolymerized and the delaminated surfaces were studied by angle-resolved XPS. Effective photografting and photolamination between two LDPE films can be achieved under atmospheric conditions and in the complete absence of an added photoinitiator and system degassing, provided that the polymer substrates are pretreated with ozone. Both the graft yield and lamination strength depend on the chemical structure, property, and the room-temperature phase state of monomers being used. For photolamination carried out with the AAC, DMAA, and amphoteric DMAPS monomers, the lamination failure is cohesive in nature. On the other hand, for photolamination carried out with the DMAEMA, AAm, and NaSS monomers, delamination occurs via adhesional failure in the graft layer.

LA971018Z